Membranes of Cationic Gemini Lipids based on Cholesterol with Hydroxyl Headgroups and their Interactions with DNA and Phospholipid

ARTICLE *in* THE JOURNAL OF PHYSICAL CHEMISTRY B · JANUARY 2011

Impact Factor: 3.3 · DOI: 10.1021/jp108372z · Source: PubMed

3 AUTHORS, INCLUDING:

Joydeep Biswas
Sikkim Manipal Institute of Technology
10 PUBLICATIONS **131** CITATIONS

SEE PROFILE

Santanu Bhattacharya
Indian Institute of Science
238 PUBLICATIONS **6,667** CITATIONS

SEE PROFILE

Membranes of Cationic Gemini Lipids based on Cholesterol with Hydroxyl Headgroups and their Interactions with DNA and Phospholipid

Joydeep Biswas,[†] Avinash Bajaj,[†,||] and Santanu Bhattacharya*[,†,‡,§]

Department of Organic Chemistry, Indian Institute of Science, Bangalore 560 012, India, Chemical Biology Unit of JNCASR, Bangalore 560 064, India, and J. C. Bose Fellow, DST, New Delhi, India

Received: September 2, 2010; Revised Manuscript Received: November 14, 2010

Two series of cholesterol-based cationic gemini lipids with and without hydroxyl functions at the headgroups possessing different lengths of polymethylene [$-(CH_2)_n-$] ($n = 3, 4, 5, 6, 12$) spacer have been synthesized. Each gemini lipid formed stable suspension in water. The suspensions of these gemini lipids in water were investigated using transmission electron microscopy, dynamic light scattering, zeta potential measurements and X-ray diffraction to characterize the nature of the individual aggregates formed therein. The aggregation properties of these gemini lipids in water were found to strongly depend upon the length of the spacer and the presence of hydroxyl group at the headgroup region. Lipoplex formation (DNA binding) and the release of the DNA from such lipoplexes were performed to understand the nature of interactions that prevail between these cationic cholesterol aggregates and duplex DNA. The interactions between such gemini lipids and DNA depend both on the presence of OH on the headgroups and the spacer length between the headgroups. Finally, we studied the effect of incorporation of each cationic gemini lipid into dipalmitoyl phosphatidylcholine vesicles using differential scanning calorimetry. The properties of the resulting mixed membranes were found again to depend upon the nature of the headgroup and the spacer chain length.

Introduction

Cationic lipids have been widely employed as nonviral DNA delivery agents owing to their amenability to rational design enabling to foster a structure−function relationship.[1−3] In addition, such molecules demonstrate negligible immunogenic reactions, possess favorable safety profiles, and are convenient to scale up and administration.[4,5] These lipids typically contain one or multiple cationic headgroup(s), a lipophilic domain and an appropriate functional group that joins the hydrophobic and hydrophilic ends.[6,7] Among the various lipids that are known, cholesterol-based cationic lipids comprise an important class of molecules that finds widespread use in gene and drug delivery[8−14] often due to their less toxic nature.[15,16] Because of these advantages, there has been a growing interest in the design and syntheses of new species of cholesterol-based lipids.[17,18] Cholesterol also associates strongly with natural lipids like L-α-dipalmitoyl phosphatidylcholine (DPPC) or cationic lipids in membranes and influence the thermal properties and the permeability of the resulting covesicles.[19−23]

Of the various molecular forms of lipids, geminis are quite interesting as they possess unusual aggregation and surface properties.[24] Gemini lipids are typically made up of two lipid "monomers" connected via a spacer at the headgroup level. The aggregation behavior of such lipids strongly depends upon both the length of the spacer between the headgroups and also on the nature of the headgroup as well.[25] The ability of the cationic lipids to become useful for biological applications depends upon their aggregation properties and their interactions with biological membranes.[26,27]

It has been already reported that the linkage between the headgroup and hydrophobic part plays an important role in the gene transfection activity.[28,29] However, the gemini form of the corresponding lipid systems bearing hydroxyl at the headgroup have never been synthesized and accordingly nothing is known about their physical and biological properties. Herein we introduce two new series of ether-linked cholesterol-based cationic gemini lipids with and without hydroxyl functions at the headgroups (Figure 1). Within each series, the lipid molecules differ in the length of the polymethylene spacers that connect the two headgroups. The lipids possessing OH functions at the headgroups were shown to be ∼2−3-fold more efficient in transfection than the corresponding lipids with no OH groups.[30] Moreover, the transfection efficiency of the hydroxyalkyl lipids decreased as the chain length of the hydroxyalkyl group increased. For comparison we also included here the corresponding gemini lipids devoid of OH group (**CG** series). We have examined the individual lipid aggregates using negative-stain transmission electron microscopy (TEM) to discern the morphologies formed from each lipid upon aggregation in water. Dynamic light scattering (DLS) was used to determine their hydrodynamic diameter. X-ray diffraction (XRD) studies of the cast films from the lipids afforded the bilayer widths of the aggregates.

Study of the interactions of cationic lipids with the natural phospholipids, for example, DPPC in mixed membranes, provides useful insights into the cationic lipid−phospholipid interactions.[26] Cationic cholesterol derivatives should alter the phospholipid-based membrane packing and also modify the membrane surface charge characteristics. While there are reports that examine the interaction of the natural cholesterol and phosphatidylcholine lipids in membranes,[31−42] there has been no attempt to examine the effect of cationic cholesterol-based

* To whom correspondence should be addressed. E-mail: sb@orgchem.iisc.ernet.in. Phone: (91)-80-2293-2664. Fax: (91)-80-2360-0529.
† Indian Institute of Science.
‡ Chemical Biology Unit of JNCASR.
§ J. C. Bose Fellow, DST.
|| Present Address: Regional Centre for Biotechnology, 180 Udyog Vihar, Phase 1, Gurgaon 122016, India.

10.1021/jp108372z
Published on Web 12/30/2010

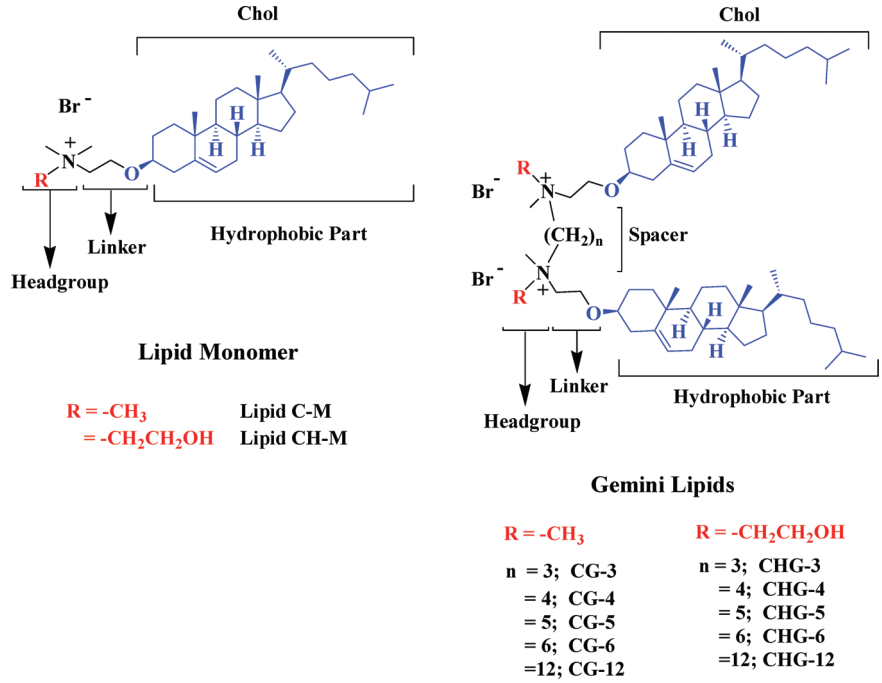

Figure 1. Molecular structures of nonhydroxylated and hydroxylated cationic cholesterol-based gemini lipids and their monomeric counterparts used in the present investigation.

gemini lipids on the physical chemical properties of DPPC membranes. Accordingly, we examined the effect of incorporation of different cholesterol-based cationic gemini lipids of two series with membranes of a natural phospholipid, DPPC using high sensitivity differential scanning calorimetry (DSC). Each cholesterol-based lipid depressed the thermal phase transition temperature of the DPPC membranes, although the extent of variation of various thermal parameters was dependent on the cholesterol lipid type and the amount of it included in the mixed membranes. Using an ethidium bromide based exclusion assay,[43] we determined the extent of DNA binding of each cholesterol-based cationic gemini lipid (lipoplex formation). We also studied the DNA release from such lipoplexes upon addition of anionic SDS (sodium dodecyl sulfate) solution. A comparative analysis of the DNA dissociation from lipoplexes induced by SDS micelles provided a relationship between such activity and the molecular structure of the individual gemini lipid. Thus in the present study, we show how various physical parameters vary when cationic gemini lipid membranes based on cholesterol interact with DNA (binding and dissociation) and naturally occurring DPPC membranes (model animal cell membranes). These observations have important bearing in understanding the gene transfection potential of these newly developed lipid molecules.

Experimental Section

Materials and Methods. All reagents, solvents, and chemicals used in this study were of the highest purity available. The solvents were dried prior to use. Column chromatography was performed using 60−120 mesh silica gel. NMR spectra were recorded using a Jeol JNM λ−300 (300 MHz for ^{1}H and 75 Hz for ^{13}C) spectrometer. The chemical shifts (δ) are reported in parts per million downfield from the internal standard, TMS, for ^{1}H NMR and ^{13}C NMR. Mass spectra were recorded on a Kratos PCKompact SEQ V1.2.2 MALDI-TOF spectrometer, a MicroMass ESI-TOF spectrometer. Infrared (IR) spectra of neat samples were recorded on a Jasco FT-IR 410 spectrometer. Calf thymus (CT) DNA was purchased from Sigma and was used as received. Gemini lipids were characterized fully by their ^{1}H NMR, ^{13}C NMR, mass spectra, and elemental analysis as described in the Supporting Information.

Liposome Preparation. Each cationic lipid was dissolved in chloroform in Wheaton glass vials. Thin lipid film was made by evaporating the organic solvent under a steady stream of dry nitrogen. The last traces of organic solvent were removed by keeping these films under vacuum for 4−5 h. Freshly autoclaved water (Milli-Q) was added to individual film such that final concentration of the cationic lipid was ∼1 mM. The lipids mixed with water were kept at 4 °C for ∼10 h for hydration and were repeatedly freeze−thawed (ice cold water to 70 °C) with intermittent vortexing to ensure hydration. Sonication of these suspensions in a bath sonicator at 70 °C for 15 min afforded cationic liposomes. When kept under strictly sterile conditions, the liposomes were found to be stable even beyond 1 month.

Dynamic Light Scattering and Zeta Potential Measurements. Lipid suspensions (1 mM) prepared in water (as mentioned above) were diluted to 0.33 mM and were used for dynamic light scattering studies. Particle size measurements of each lipid aggregate were performed at room temperature with a Malvern Zetasizer Nano ZS particle sizer (Malvern Instruments Inc., MA), which employed an incident laser beam of 633 nm wavelength. Mean diameters reported were obtained from Gaussian analysis of the intensity-weighted particle size distributions. Zeta potential measurements for each lipid suspension were performed at ambient temperature using an applied voltage of 50 mV. Electrophoretic mobility was measured by the Laser Doppler Velocimetry technique and converted by the instrument software (Dispersion Technology Software 5.02, Macromedia, Inc.) to zeta potential. Henry equation[43] was used to calculate the zeta potentials from the measurement of electrophoretic mobility assuming the viscosity of the dilute lipid suspensions to be the same as water.

Transmission Electron Microscopy. A 10 μL sample of each lipid suspension was loaded onto Formvar-coated, 400 mesh copper grids and allowed to remain for 1 min. Excess fluid was removed from the grids by touching their edges with filter paper and 10 μL of 0.1% uranyl acetate was applied on the same grid after which the excess stain was similarly removed from the grids. Each sample-containing grid was air-dried and then the last traces of water were removed under vacuum and finally examined using TEM (TECNAI F30) operating at an acceleration voltage (DC) of 100 keV and the micrographs were recorded at a magnification of 4000−20000.

Lipid Cast-Film X-ray Diffraction. Following reported procedures,[44,45] aqueous aggregates of each lipid (1 mM) were placed on a precleaned glass slide that upon air-drying afforded a thin film of the particular lipid aggregate on the glass plate. XRD of an individual cast film was performed using the reflection method using a Phillips (X'pert PRO) X-ray diffractometer. The X-ray beam was generated using a Cu anode and a Cu−Kα_1 beam of wavelength 1.5418 Å. Scans were performed for 2θ values up to 14° with a scan rate of 0.5° per min and a step size of 0.02°.

Differential Scanning Calorimetry (DSC). Thermotropic properties of the individual lipid aggregates in water were investigated by high-sensitivity DSC using a CSC-4100 multicell differential scanning calorimeter (Calorimetric Sciences Corporation, Utah, U.S.A.).[46−49] DPPC (amount fixed) mixed with the desired quantity of each of the cholesterol-based cationic lipid was dissolved in chloroform in Wheaton glass vials to afford the desired mol % cationic lipid-DPPC mixtures. Each thin film was made from specific lipid mixtures by evaporating the organic solvent under a steady stream of dry nitrogen. The last traces of organic solvent were removed by keeping these films under vacuum for 4−5 h. Freshly autoclaved water (Milli-Q) was added to the individual film such that final concentration of the DPPC-cationic lipid coliposome was ∼1 mM (with respect to DPPC). Each DPPC-cationic lipid mixture in water was kept at 4 °C for ∼10 h for hydration and was repeatedly freeze−thawed (ice cold water to 70 °C) with intermittent vortexing to ensure optimal hydration. Sonication of each suspension in a bath sonicator at 70 °C for 15 min afforded DPPC-cationic lipid coliposomes, each of which (0.5 mL) was carefully transferred into separate DSC ampule and then the ampules were screw-capped tightly. The measurement was carried out in the temperature range of 20−70 °C at a scan rate of 20 °C/h. At least two consecutive heating and cooling scans were performed. Baseline thermograms were obtained using the same amount of the degassed Milli-Q water in the respective DSC cells. The thermograms for the lipid aggregate samples were obtained by subtracting the respective baseline thermogram from the sample thermogram using "CpCalc" software. From the plot of excess heat capacity versus temperature, solid gel-to-liquid-crystalline transition temperature (T_m), enthalpy (ΔH_c) and entropy (ΔS) of the transitions were obtained. The size of the cooperativity unit (CU) for the melting transition was determined using the formula, CU = ($\Delta H_{vH}/\Delta H_c$) where the ΔH_{vH} is the van't Hoff enthalpy and the ΔH_c is the calorimetric enthalpy.[49] The van't Hoff enthalpy was calculated from the equation $\Delta H_{vH} = 6.9\ T_m^2/\Delta T_{1/2}$, where T_m is the phase transition temperature and $\Delta T_{1/2}$ is the full width at half-maximum of the thermogram.[50]

Ethidium Bromide Displacement Assay. Fluorescence emission due to 2.5 μM ethidium bromide (EB) at 592 nm (keeping the slit widths fixed at 10 nm for both excitation and emission) was first measured in 5 mM HEPES, 0.1 M NaCl, pH 7.4 buffer. To this CT-DNA (4.0 μM base molarity) was added and enhancement emission due to EB upon intercalation into duplex DNA was measured at 37 °C. This titration was continued until saturating concentration of CT-DNA was added to obtain maximum fluorescence emission. Then an aliquot of a given cationic liposome (0.8 μM) was added into the preformed EB/CT-DNA complex in 5 mM HEPES (pH 7.4) buffer. This resulted in a fluorescence quenching due to the displacement of EB molecules from the intercalated sites caused due to distortion in DNA double-helix upon addition of cationic lipid aggregates. Progressive addition of an aqueous solution of sodium dodecyl sulfate (SDS) to above cationic lipid/DNA complex (lipoplex) resulted in the release of DNA from the lipoplexes. Upon release of DNA, EB reintercalated into it and the fluorescence emission increased. If F_0 is the fluorescence intensity (FI) of unintercalated EB, F_{max} is the FI of the fully intercalated EB and F_x is the FI for EB upon addition of a given concentration of lipid or SDS, then

$$\%\mathrm{FI} = (F_x - F_0)/(F_{max} - F_0) \quad (1)$$

Using eq 1, we determined the ability of each lipid to complex with DNA and SDS induced dissociation of various lipoplexes.

Results and Discussion

Lipids. We have synthesized 10 new gemini lipids and their corresponding monomeric lipids differing in their headgroups and the spacer that separates the two headgroups (Supporting Information). Compound **1** was subjected to a reaction with *p*-toluenesulfonyl chloride in pyridine-chloroform (v/v: 1/1) for 6 h at 0 °C to get **2** in 88% yield. Then the compound **2** was treated with either *N*-methylethanolamine or *N*,*N*-dimethylamine in dry CH_3CN under refluxing conditions to produce **4** and **5**, respectively. The hydroxylated cholesterol-based gemini lipids (**CHG**) were synthesized from the precursor cholest-5-en-3β-oxyethan-*N*-methyl-*N*-2-hydroxyethylamine (**4**) by reacting it with the corresponding α,ω-dibromoalkanes in 40−50% yields. Nonhydroxylated cholesterol-based gemini lipids (**CG**) were synthesized from the precursor cholest-5-en-3β-oxyethan-*N*,*N*-dimethylamine (**5**) by reacting it with corresponding α,ω-dibromoalkanes as reported previously.[10] Each gemini lipid was purified by repeated crystallizations from a mixture of MeOH and EtOAc. Each new cholesterol-based cationic gemini lipid was characterized fully by ^{1}H NMR, ^{13}C NMR, ESI-MS, and elemental analysis. The monomeric lipids **CH-M** and **C-M** were synthesized as reported earlier.[28,51]

Lipid Aggregates. Stable suspension of each lipid in aqueous media was prepared by brief vortexing followed by bath sonication of hydrated thin films of individual lipids at 35 W for 15 min at 70 °C. Each cationic gemini lipids formed clear suspension in aqueous media and all of them were optically stable even after one month when stored at 4 °C under sterile conditions.

Transmission Electron Microscopy. Each lipid, the molecular structure of which is shown in Figure 1, formed approximately globular aggregate substructures in water as evident from the negatively stained TEM. Representative TEM images are shown in the Figure 2. Typical diameters of the sonicated lipid aggregates varied from 20 to 160 nm in diameters for the nonhydroxylated cationic cholesterol gemini lipids (**CG**). While the aggregates seen under TEM for the nonhydroxylated series of monomeric (**C-M**) and gemini lipids (**CG-3**, **CG-6** and **CG-12**) are of variable sizes, all of them appear like typical vesicular

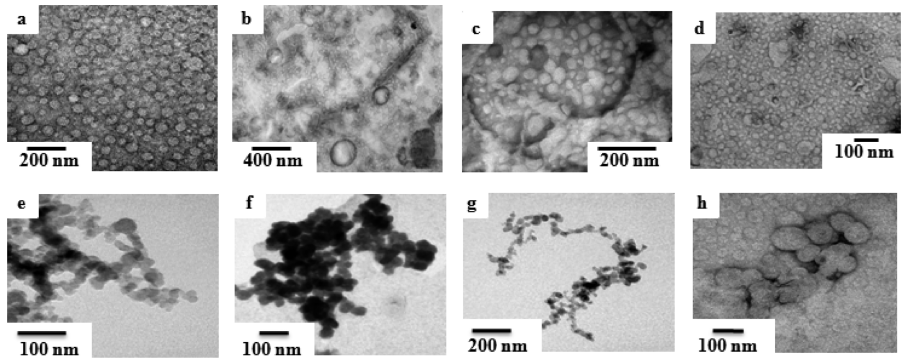

Figure 2. Negative-stain transmission electron micrographs of aqueous suspensions of the nonhydroxylated cholesterol-based cationic lipids (a) **C-M**, (b) **CG-3**, (c) **CG-6**, and (d) **CG-12** and that of the hydroxylated cholesterol-based cationic lipids (e) **CH-M**, (f) **CHG-3**, (g) **CHG-6**, and (f) **CHG-12**.

TABLE 1: Average Hydrodynamic Diameters of the Lipid Aggregates As Obtained from DLS Measurements, Size of the Aggregates Obtained from TEM Studies and Bilayer Width of the Aggregates of Cholesterol-Based Cationic Gemini Lipids

lipids	hydrodynamic diameter (nm)[a]	size From TEM (nm)[b]	bilayer width (Å)[c]	zeta potential (mV)
C-M	140 ± 1	50−80	48.4	35 ± 2
CG-3	120 ± 8	40−60	45.6	40 ± 3
CG-4	151 ± 3	80−110	45.7	61 ± 3
CG-5	101 ± 2	30−50	46.7	45 ± 4
CG-6	148 ± 1	70−130	45.9	68 ± 4
CG-12	134 ± 1	40−90	46.7	61 ± 3
CH-M	51 ± 1	20−40	49.7	40 ± 3
CHG-3	113 ± 2	30−60	46.6	44 ± 3
CHG-4	151 ± 1	50−70	46.6	57 ± 1
CHG-5	207 ± 7	80−150	46.7	62 ± 4
CHG-6	152 ± 4	50−90	46.7	61 ± 1
CHG-12	225 ± 1	100−120	46.8	64 ± 4

[a] Hydrodynamic diameters obtained from DLS measurements. [b] As evidenced from TEM. [c] Unit bilayer thickness from XRD experiments.

structures (Figure 2a−d). For the corresponding hydroxylated series of lipids (**CHG**), suspensions of both monomeric lipids (**CH-M**) and their gemini counterparts were found to form "connected" and aggregated conglomerates of vesicles of different length scales (Figure 2e−h). This could have been caused by the hydrogen bonding interactions imposed by the hydroxyethylated headgroups of the lipids of each vesicle of this type of cholesterol derivatives. The sizes of the vesicles obtained from TEM were generally found to be less than those obtained from the DLS studies of each cationic gemini lipid of the two series (see below). Such reduction in size observed under TEM could be because of the shrinkage of the vesicles while drying before taking TEM images.[21]

Dynamic Light Scattering. The average hydrodynamic diameters of all the cholesterol-based cationic gemini lipid aggregates of the two series were determined using dynamic light scattering studies and are recorded in the Table 1. DLS experiments show that among the nonhydroxylated cholesterol-based cationic lipids, the aggregates of gemini lipid with -$(CH_2)_5$- spacer length (i.e., **CG-5**) are the smallest (∼100 nm) in hydrodynamic diameter than other lipids of the series whereas the lipid aggregates with -$(CH_2)_4$- spacer length (i.e., **CG-4**) are the largest in hydrodynamic diameter (∼150 nm). For the hydroxylated cholesterol-based cationic lipids, DLS measurements show that the lipid aggregates of **CH-M** are the smallest (∼50 nm) in hydrodynamic diameter among the lipids of the series whereas the lipid aggregates with -$(CH_2)_{12}$- spacer length (**CHG-12**) are the largest in hydrodynamic diameter (∼225 nm). Among the two monomers, monomeric lipid aggregates **C-M** were larger in hydrodynamic diameter than the corresponding hydroxylated monomeric lipid aggregates **CH-M**.

Zeta Potential Measurements. Each cholesterol-based cationic lipid aggregate of either series was further characterized by measuring the zeta potential of their suspensions in water. This allowed determination of the effective surface charge of the exposed surface of the lipid aggregates in aqueous media. Relevant data are shown in Table 1. Among the nonhydroxylated cholesterol-based cationic lipid aggregates, the zeta potential of the lipid aggregate **CG-6** (∼68 mV) was found to be the highest whereas the zeta potential for the monomeric lipid aggregate **C-M** (∼35 mV) was found to be the lowest. In the case of hydroxylated cholesterol-based cationic lipid aggregates, the lipid aggregate **CHG-12** (∼64 mV) was found to have the highest zeta potential value whereas the lipid aggregate **CH-M** (∼40 mV) had the lowest zeta potential value. Notably, lipid **CG-6** formed aggregates of the highest zeta potential value in the series when dispersed in water among the entire cholesterol-based cationic gemini lipids whereas **CHG-12** formed aggregates of the highest zeta potential value among the hydroxylated cholesterol-based cationic gemini lipid series. Thus compared to the monomeric lipids the zeta potential was found to be significantly higher for the corresponding gemini lipid aggregates. Interestingly introduction of hydroxyl group at the headgroup did not however, influence the zeta potential so much.

X-ray Diffraction Studies. X-ray diffraction experiments of the self-supported cast films of the aqueous suspensions of each of the cholesterol-based cationic lipids showed a series of higher order reflections characteristic of lamellar phases in their diffraction pattern. The bilayer widths were determined from the Bragg's equation ($n\lambda = 2d \sin \theta$) and the corresponding data for each lipid of the two series are given in the Table 1. Among the two series of cholesterol-based cationic lipids, the monomeric lipids, that is, **C-M** and **CH-M**, were found to have the longer bilayer widths than that of their gemini lipid counterparts. Incorporation of the $-(CH_2)_n-$ spacer at the headgroup region joining two monomeric units lowered the bilayer thicknesses of the two series of lipid aggregates compared to the theoretical values obtained from twice the lengths of their energy-minimized conformational drawings. Accordingly, the monomeric lipids (**C-M** and **CH-M**) appear to form nearly regular bilayer type arrangements whereas gemini lipids most likely form interdigitated and tilted bilayer arrangements as depicted in Scheme 1. The widths of the aggregates of the CHG series cholesteryl lipids were ∼1 Å longer than their nonhydroxylated counterparts. However, as the spacer

SCHEME 1: Differences in the Molecular Packing in Bilayer Arrangements of Cholesterol-Based Cationic Monomeric Lipid and Gemini Lipid

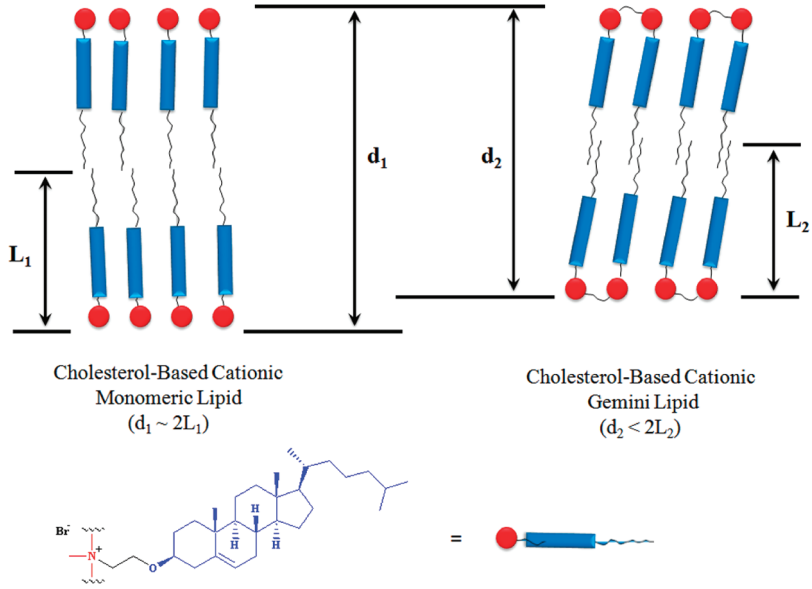

chain lengths in the corresponding gemini lipids increase, such small differences disappear. It appears that the insertion of longer polymethylene chains in geminis counterbalances the effect of OH group incorporation at the headgroup.

Differential Scanning Calorimetry. Dipalmitoyl phosphatidyl choline (DPPC) or their mixtures with individual cationic cholesteryl lipids at defined ratios were dispersed in water (Milli-Q) using a vortex mixing procedure, followed by five freeze−thaw cycles. Well-defined thermal phase transitions were observed from each sample that contained DPPC while the individual cholesteryl lipid dispersions did not show any transition irrespective of their molecular structures as expected. Addition of cationic gemini cholesterol lipids caused progressive broadening of the gel-to-liquid-crystalline phase transition of DPPC leading to its eventual abolition at higher concentrations of the former (Figure 3). However, the concentrations of the cholesterol-based cationic lipids required for the complete abolition of the phase transition varied significantly as compared to that of natural cholesterol. For instance, nearly 45 mol % of cholesterol is required to completely quench the chain motions of DPPC resulting in total abolition of phase transition.[52] In contrast, only 10 mol % of the gemini cholesterol lipids was enough to nearly completely abolish the phase transition of DPPC. For the corresponding monomers, however, more than 10 mol % was required for the abolition of the phase transition of DPPC. We observed greater extent of broadening of the phase transition profile of DPPC membranes that contained 10 mol % of **C-M** as compared to that of hydroxylated **CH-M**. At 10 mol % of each cationic lipid-doped DPPC vesicles, only the ones with **CG-3** showed a small but an observable phase transition. Maximum broadening of the DPPC transition peak was observed in the case of gemini lipids, **CHG-6** and **CHG-12**.

The thermal phase transition properties for the DPPC coaggregates of each of the two series of cholesterol-based cationic gemini lipids are summarized in Table 2. The main-chain phase transition temperature T_m is the temperature at which the membranous aggregates are half converted to the fluid phase. In the case of both cholesterol-based cationic gemini lipids devoid of OH function and the ones with OH appended headgroups, their incorporation into DPPC membranes led to the depression of the transition temperature of the DPPC bilayers. This was true irrespective of whether the spacer was short or long, but the effectiveness in broadening the melting transition was invariably higher with the geminis compared to their monomeric counterparts (**C-M** or **CH-M**). Also the progressive broadening of the melting transition of DPPC increased with an increase in the spacer-chain length of the gemini lipids of either series. It may be noted that the effect of incorporation of cholesterol-based lipids on the thermal phase transition of DPPC did not differ in any significant way whether a OH group is included at the level of headgroup of the former. The melting transition of DPPC was virtually abolished upon inclusion of 10 mol % of gemini lipids while >10 mol % of **C-M** was necessary for complete abolition of the melting process. In most cases, the calorimetric enthalpy (ΔH_c) that was associated with the chain melting of the palmitoyl chains in DPPC/lipid coaggregates was significantly lower than that of pure DPPC membranes as addition of cholesterol-based cationic lipids into DPPC led to progressive broadening of the phase transition of DPPC leading to its eventual abolition. Transition enthalpy, entropy, and cooperativity unit values generally decreased with an increase in the amount of cholesterol-based cationic gemini lipids included in the coaggregates of DPPC. These observations are consistent with progressive broadening of DPPC phase transition with the inclusion of cholesterol-based lipids.

In an earlier investigation,[52] it has been shown that unlike natural cholesterol, the cationic lipids based on cholesterol depress the melting temperature (T_m) of the DPPC bilayers. Here in case of the cationic cholesterol gemini lipids, the depression in the melting temperatures was found to depend on the % of gemini cholesterol lipid included in the DPPC membranes. These gemini cholesterol lipids retain the property of cholesterol in that they function as "filler" molecules within the bilayer interacting with the neighboring DPPC molecules. This is why these lipids could quench the motions of the palmitoyl chains of DPPC and broaden the thermal phase transition eventually abolishing the phase transition.

The changes in the shape of the peak due to phase transition for a particular coaggregate indicate compositional variations during phase transition. It is reasonable to assume that upon

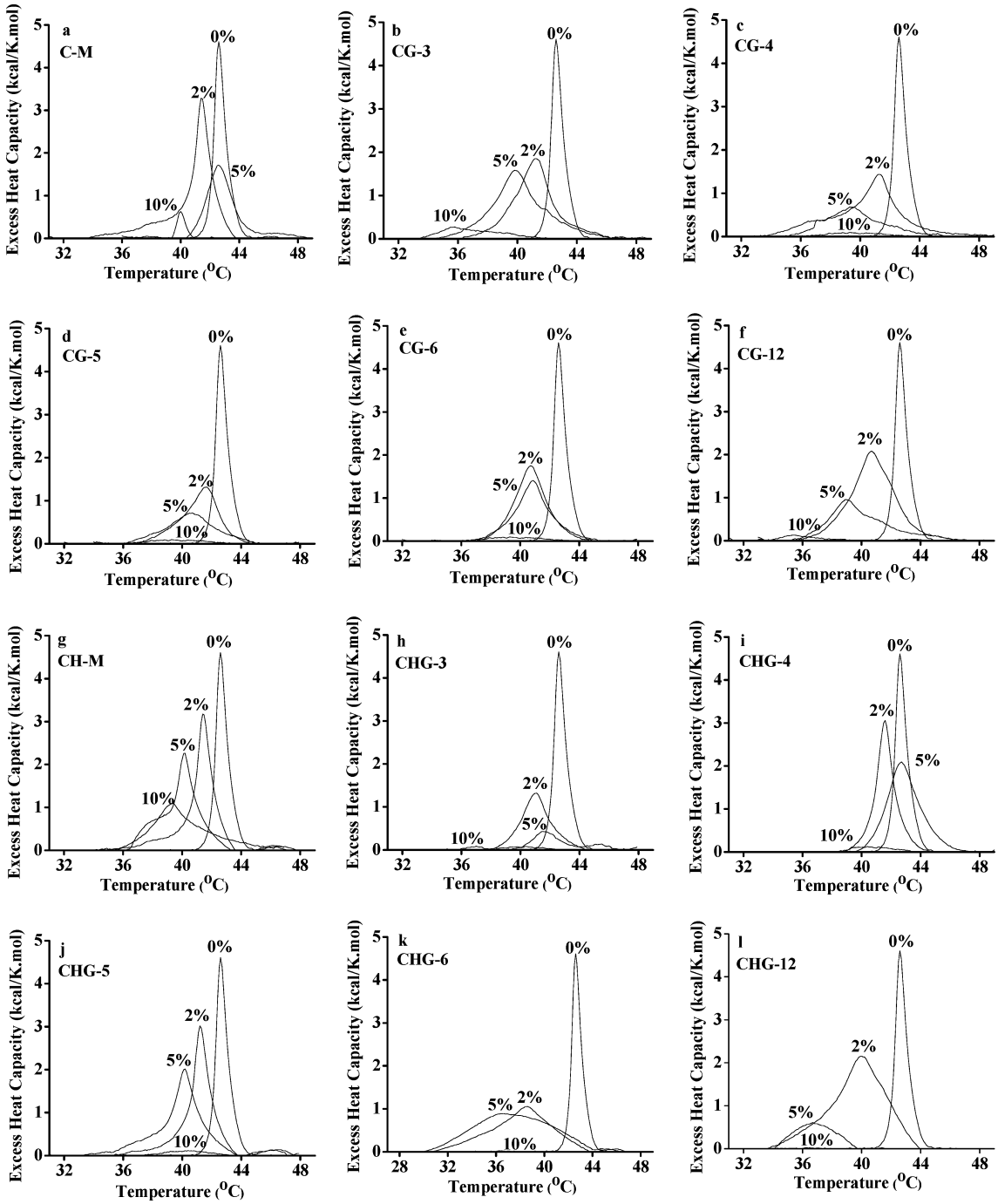

Figure 3. Differential scanning calorimetry profiles of the multilamellar vesicles of DPPC doped with an indicated mol % of cholesterol-based cationic lipids (a) **C-M**, (b) **CG-3**, (c) **CG-4**, (d) **CG-5**, (e) **CG-6**, (f) **CG-12**, (g) **CH-M**, (h) **CHG-3**, (i) **CHG-4**, (j) **CHG-5**, (k) **CHG-6**, and (l) **CHG-12**.

incorporation they form domains rich in DPPC (which show a sharp peak) and domains that are rich in cholesterol-based gemini lipids (which appear as a broadened peak).[52] The sharp peak due to the melting of DPPC is strongly affected by an increasing concentration of the gemini lipids in terms of enthalpy and position. One may assign this peak due to the thermal transition of a "DPPC-rich" domain. Further addition of the cholesterol-based cationic gemini lipids serves mainly to convert the DPPC-rich population into a "DPPC-poor" population. The DPPC-poor population may be responsible for the peak broadening. Each cationic lipid has slightly different mode and strength of interaction with DPPC; this is reflected in the change in position and shape of the sharp peak due to formation of a different entity of DPPC and cholesterol-based gemini lipids. The formation of a broad and a sharp peak due to cholesterol-poor and cholesterol-rich phases, respectively, due to incorporation of cholesterol in DPPC and other lipids has indeed been observed with natural cholesterol also.[52]

DNA Complexation by Cationic Cholesterol Aggregates. The effect of addition of each cationic cholesterol aggregates to calf-thymus DNA (CT-DNA) was investigated to compare their efficiency of lipoplex formation. For this, fluorescence spectral measurements were made by exposing CT-DNA (4.0 μM) to 2.5 μM ethidium bromide (EB), which is a known DNA intercalator. While the fluorescence emission due to free EB is very low in water, the fluorescence maximizes with a peak at 592 nm when all the EB molecules occupy the DNA duplex. Progressive addition of a given cationic cholesterol-based

TABLE 2: Thermodynamic Properties of the Phase Transition of DPPC Membranes and Its Coaggregates with Cholesterol-Based Cationic Lipids As Determined from Differential Scanning Calorimetry[a]

lipids	% in DPPC[a]	T_m[b] (°C)	ΔH_c[c] (kcal/mol)	ΔS[c] (cal/K·mol)	CU[d]
DPPC		42.6	7.1	22	144
C-M	2	41.4	6.4	20	104
	5	42.6	3.9	12	*e*
	10	40.0	0.5	1	*e*
CG-3	2	41.2	5.9	19	112
	5	39.8	6.2	20	98
	10	35.8	1.2	4	*e*
CG-4	2	41.3	6.1	19	87
	5	39.3	2.9	9	*e*
	10	*n*			
CG-5	2	41.7	3.8	12	154
	5	40.7	2.7	9	*e*
	10	*n*			
CG-6	2	40.7	4.6	15	109
	5	40.9	4.0	13	*e*
	10	n			
CG-12	2	40.7	7.3	23	76
	5	38.9	3.9	12	*e*
	10	*n*			
CH-M	2	41.4	5.6	18	115
	5	40.2	5.3	17	107
	10	39.3	4.2	14	*e*
CHG-3	2	41.1	3.2	10	139
	5	41.5	1.3	4	*e*
	10	*n*			
CHG-4	2	41.6	5.0	16	121
	5	42.7	5.7	18	101
	10	*n*			
CHG-5	2	41.2	5.7	18	67
	5	40.2	5.7	18	49
	10	*n*			
CHG-6	2	38.6	6.1	20	91
	5	36.6	7.2	23	76
	10	*n*			
CHG-12	2	40.0	9.1	29	71
	5	36.7	0.8	3	28
	10	*n*			

[a] See text for experimental details on DSC; [DPPC] = 1 mM; scan rate used was 0.5 K/min. [b] Main transition peak that was observed. Accuracy of T_m was ±0.2 °C between successive runs of the same sample; two different sample preparations gave a difference of ±1.5 °C; "*n*" signifies that no detectable phase transition was observed. [c] Calorimetric data are averages of two independent experiments where the error in ΔH_c is ±0.2 kcal/mol and the error in ΔS is ±0.001 cal/K·mol. [d] Size of the co-operativity unit (CU). [e] It was not possible to determine CU accurately due to the complex nature transitions.

aggregate into the EB/DNA complex led to a gradual quenching of the fluorescence emission eventually leading to saturation as shown in the Figure 4C,D for nonhydroxylated and hydroxylated cholesterol-based cationic lipids, respectively. Quenching of the fluorescence intensity at 592 nm upon addition of cationic cholesterol lipid suspensions takes place due to the gradual release of "free" EB out of DNA (Figure 4A, for lipid **C-M**). This occurs because cationic cholesterol aggregates form lipoplexes with DNA (compaction), leading to the dissociation of EB from the EB-DNA complex. The percentage decreases of FI (FI %) until saturation for the given lipid suspension depended on the molecular structure of the cationic lipid (insets, Figure 4C,D). Figure 4C,D further shows how various cholesterol-based cationic gemini lipid suspensions promote dissociation of EB from EB/DNA complexes at various lipid-to-DNA charge ratios.

From the ethidium bromide exclusion assay, we find that among the nonhydroxylated cationic cholesterol aggregates, the monomeric **C-M** liposomes are more efficient in binding to DNA than their gemini counterparts. The aggregates of monomeric **C-M** induce the dissociation of EB from the EB/DNA complex to an extent of ∼93% at a maximum lipid/DNA ratio 3.0. The DNA−lipid complexation is almost complete at lipid/DNA ratio of 2.0 for lipid **C-M**. In contrast the aggregates of gemini lipids, for example, **CG-4** and **CG-12** showed lower extent of EB exclusion (∼74%) from the EB/DNA complex in this series (Figure 4C). In the case of the gemini lipids, the saturation of lipid/DNA complexation was more gradual leading to a maximum complexation at lipid to DNA ratio of ∼3.0.

In the case of the hydroxylated cholesterol-based cationic lipid series, monomeric **CH-M** liposomes were also found to be the best in binding to DNA as compared to their gemini lipid counterparts in the series. The **CH-M** aggregates facilitate the release of EB from the EB/DNA complex to an extent of ∼81%. Among the geminis of the hydroxylated series, the aggregates of **CHG-6** show the maximum binding with DNA whereas the **CHG-3** liposomes show the least binding with DNA (Figure 4D). The aggregates of monomeric **C-M** show the highest binding with the DNA among all the cholesterol-based cationic lipids of the two series examined here.

Perhaps insertion of a polymethylene segment in the geminis imposes a restriction in their freedom toward binding with duplex DNA compared to the monomeric counterparts. Also the incorporation of a hydroxyethyl at the headgroup brings down the propensity of its lipoplex formation with DNA. This may be due to the extra hydration experienced by the gemini lipids having the OH groups that shield these cationic cholesterol aggregates from facile lipoplex formation with DNA. Lipoplex formation, although driven by the attractive Coulombic forces between cationic lipids and DNA, is also accompanied by the release of "ordered" water molecules from the spine of hydration of DNA.[53] In the case of the hydrated cationic cholesterol aggregates (**CH-M** and **CH-G**), the entropic gain through the release of ordered water molecules from DNA may be reduced by the additional hydration experienced by the cationic hydroxyethylated cholesterol aggregates compared to their lipid counterparts without OH group.

SDS-Induced Release of DNA from Cationic Liposome-DNA Complexes. During cationic liposome-mediated gene transfection, DNA bound lipoplexes undergo DNA release via their dissociation at the endosomal cell surfaces, which are rich in negatively charged lipids.[53] To model this situation, we have used negatively charged SDS micelles to induce release of DNA from various cationic cholesterol aggregates-DNA complexes. An aqueous solution of EB (2.5 μM) gave a broad λ_{max} at 592 nm when excited at 526 nm. In the presence of saturating concentration of CT-DNA (4.0 μM base molarity), the FI at 592 nm due to intercalated EB increased more than 5-fold (Figure 4A,B). Addition of a given cationic gemini cholesterol aggregate to EB/DNA complex results in fluorescence quenching as discussed previously. Progressive addition of SDS to this mixture triggers dissociation of the cationic cholesterol lipids from the lipoplexes. This in turn facilitates the reintercalation of EB into CT-DNA, which is released from the lipoplex. The increase in the fluorescence intensity reached a plateau at a particular concentration of SDS for a given cationic liposome/DNA complex approximately at ∼1:1 SDS/cationic lipid charge ratio (Figure 4B, for lipid **C-M**). Further addition of SDS beyond this concentration did not result in any significant enhancement in the fluorescence recovery as shown in the Figure 5A,B.

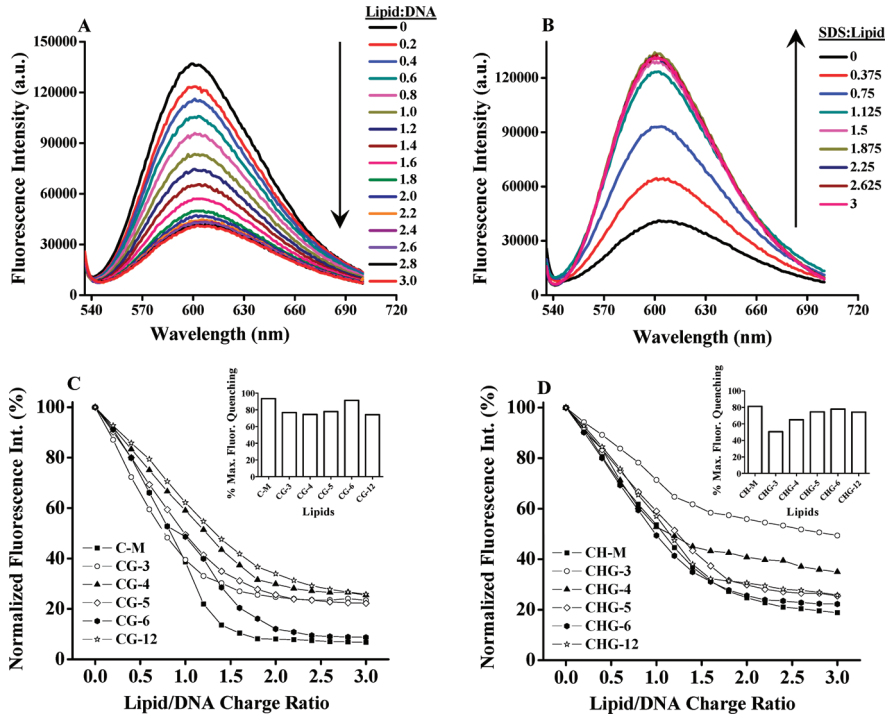

Figure 4. (A) Effect of addition of increasing amounts of cationic liposomes of **C-M** to DNA-bound EB complexes (DNA, 4 μM, base molarity). This was followed by recording the changes in fluorescence emission spectra after each addition of lipid (excitation at 526 nm and emission in the range 536−700 nm). (B) Effect of addition of SDS micelles on DNA-bound cationic liposomes (**C-M**). Release of the ethidium bromide (EB) from the DNA-EB complexes upon addition of (C) nonhydroxylated and (D) hydroxylated cholesterol-based cationic liposomes at different lipid/DNA charge ratios. Insets show % maximum fluorescence quenching vs lipids.

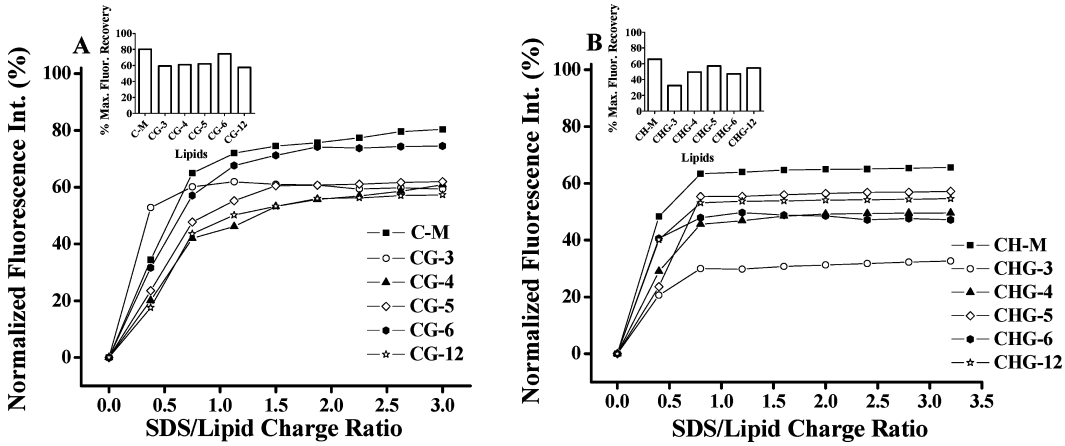

Figure 5. Reintercalation of the ethidium bromide (EB) to the duplex DNA upon the release of DNA from the cationic cholesterol lipid/DNA complexes after addition of SDS at different SDS/lipid charge ratios for (A) nonhydroxylated and (B) hydroxylated cholesterol-based cationic gemini lipids. Insets show percent maximum fluorescence recovery as a function of lipids.

In the experiments involving SDS-induced DNA release, we observe that the monomeric lipid **C-M** suspensions of the cholesterol-based cationic lipids without OH group are more efficient (∼80%) in facilitating DNA release from the lipoplex in the presence of the negatively charged micelles. In contrast for the series of cationic gemini lipids without OH group, the DNA releases observed from the respective lipoplexes were considerably lower (∼57−74%). For the hydroxylated cholesterol-based cationic lipid series also, the monomeric liposomes of **CH-M** were most effective (∼66%) in facilitating the DNA dissociation from the lipid-DNA complex in the presence of the negatively charged SDS micelles. However, the gemini lipids of the **CHG** series were more resistant to the release of DNA from their lipoplexes. Taken together the two monomeric lipids, that is, **C-M** and **CH-M** were the most efficient lipids to trigger DNA release from their lipoplexes. Conversion of monomer to gemini form of both series of lipids increases their resistance in releasing DNA from the corresponding lipoplexes in the presence of excess SDS micelles. This effect was more pronounced in the hydroxylated lipid series.

Conclusions

In this work we have introduced a series of new cholesterol-based cationic monomeric and gemini lipids with OH groups at the headgroups and studied their aggregation properties in detail. We compared the properties of the corresponding lipids without any OH groups. All monomeric and gemini lipids form stable suspensions in aqueous media. Electron microscopic studies reveal that each lipid forms nearly spherical aggregates in water. The structures seen under TEM for the nonhydroxylated series of monomeric and gemini lipids are of variable sizes, and

they appear like discrete, isolated vesicles. For the hydroxylated series of lipids, however, both the monomeric lipid aggregates (**CH-M**) and the aggregates of their gemini counterparts appear to remain "adhered" to each other to form a sort of elongated clusters of aggregates of different length scales. DLS measurements show that the suspensions of gemini **CHG-4** have the smallest hydrodynamic diameter among all the lipids. XRD studies with the cast films of lipids reveal that the monomeric lipids of either series have higher bilayer widths than the corresponding gemini lipids. The monomeric lipids (**C-M** and **CH-M**) form tilted bilayer aggregates whereas the gemini lipids form regular bilayer arrangements in their aggregates.

Calorimetry studies of the coaggregates of the cationic cholesterols with DPPC show that ~10 mol % of most of the cholesterol geminis are enough to abolish the phase transition of the DPPC membranes whereas more than 10 mol % are required for their monomeric counterparts. Further, these thermotropic properties depend upon the length of the spacer of the gemini lipid included in the mixture. We have observed greater quenching of the thermal phase transition of DPPC membranes with 10 mol % of **C-M** as compared to **CH-M** doped liposomes. At 10 mol % of all cationic lipid-doped DPPC covesicles, only **CG-3** doped systems show an observable phase transition. Maximum broadening of the DPPC transition peak was observed in the case of the geminis, **CHG-6** and **CHG-12**.

DNA binding and release studies show that the interactions between gemini lipids and DNA depend upon the nature of the headgroup as well as the length of the spacer between the headgroups. For the cholesterol-based cationic lipids without OH group, the monomeric **C-M** suspensions facilitate the release of EB from the EB-DNA complex to an extent of ~93% at a lipid/DNA ratio of 3.0 whereas the liposomes of **CG-4** and **CG-12** showed the lowest extent of maximum EB exclusion (~74%) from the EB-DNA complex at the same lipid/DNA ratio. For the **CHG** lipid series, the monomeric liposomes of **CH-M** facilitate the dissociation of EB from the intercalated EB-DNA complex to an extent of 81% whereas the liposomes of **CHG-3** showed the minimum binding to DNA. Thus the two monomeric lipids **C-M** and **CH-M** are more amenable to allow DNA dissociation from the corresponding lipoplexes than their respective gemini counterparts. Thus the present studies provide an understanding of the aggregation behavior of the new cationic cholesteryl lipids when OH groups are included at the headgroup. We also understand the nature of interactions between these lipids with the naturally occurring phosphatidylcholine lipids of the eukaryotic cell membranes. In addition, their mode of binding with DNA and the estimation of the susceptibility of DNA release from the corresponding lipoplexes give a reasonable idea about their gene transfection potential. Work is currently underway in our laboratory to assess these properties.

Acknowledgment. This work was supported by DST, Government of India, New Delhi, India. Joydeep Biswas and Avinash Bajaj thank the CSIR for awarding senior research fellowships.

Supporting Information Available: Preparation of each new lipid is described. This material is available free of charge via the Internet at http://pubs.acs.org.

References and Notes

(1) Bhattacharya, S.; Bajaj, A. *Chem. Commun.* **2009**, 4632.
(2) Kaneda, Y.; Tabata, Y. *Cancer Sci.* **2006**, *97*, 348.
(3) Ridge, K. D.; Bhattacharya, S.; Nakayama, T. A.; Khorana, H. G. *J. Biol. Chem.* **1992**, *267*, 6770.
(4) Wang, L.; MacDonald, R. C. *Gene Ther.* **2004**, *11*, 1358.
(5) Ilies, M. A.; Balaban, A. T. *Exp. Opin. Ther. Pat.* **2001**, *11*, 1729.
(6) Zhi, D. F.; Zhang, S. B.; Wang, B.; Zhao, Y. N.; Yang, B. L.; Yu, S. J. *Bioconjugate Chem.* **2010**, *21*, 563.
(7) Gao, H.; Hui, K. M. *Gene Ther.* **2001**, *8*, 855.
(8) Tagami, T.; Barichello, J. M.; Kikuchi, H.; Ishida, T.; Kiwada, H. *Int. J. Pharm.* **2007**, *333*, 62.
(9) Al-Jamal, W. T.; Kostarelos, K. *Int. J. Pharm.* **2007**, *331*, 182.
(10) Bajaj, A.; Kondiah, P.; Bhattacharya, S. *J. Med. Chem.* **2007**, *50*, 2432.
(11) Bajaj, A.; Kondaiah, P.; Bhattacharya, S. *J. Med. Chem.* **2008**, *51*, 2533.
(12) Bhattacharya, S.; Thomas, M. *Tetrahedron Lett.* **2001**, *42*, 3499.
(13) Vigneron, J. P.; Oudrhiri, N.; Fauquet, M.; Vergely, L.; Bradley, J. C.; Basseville, M.; Lehn, P.; Lehn, J.-M. *Proc. Natl. Acad. Sci. U.S.A.* **1996**, *93*, 9682.
(14) Gao, X.; Huang, L. *Biochem. Biophys. Res. Commun.* **1991**, *179*, 280.
(15) Lv, H.; Zhang, S.; Wang, B.; Cui, S.; Yan, J. *J. Controlled Release* **2006**, *114*, 100.
(16) Xu, L.; Anchordoquy, T. *Biochim. Biophys. Acta* **2008**, *1778*, 2177.
(17) Kim, B.-K.; Doh, K.-O.; Nam, J. H.; Kang, H.; Park, J.-G.; Moon, I.-J.; Seu, Y.-B. *Bioorg. Med. Chem. Lett.* **2009**, *19*, 2986.
(18) Bajaj, A.; Kondaiah, P.; Bhattacharya, S. *Bioconjugate Chem.* **2008**, *19*, 1640.
(19) Demel, R. A.; Lala, A. K.; Nanda Kumari, S.; Van Deenen, L. L. M. *Biochim. Biophys. Acta* **1984**, *771*, 142.
(20) Franova, M.; Repakova, J.; Capkova, P.; Holopainen, J.; Vattulainen, I. *J. Phys. Chem. B* **2010**, *114*, 2704.
(21) Benatti, C.; Epand, R.; Lamy, M. T. *Chem. Phys. Lipids* **2007**, *145*, 27.
(22) Bhattacharya, S.; Haldar, S. *Biochim. Biophys. Acta, Biomembr.* **1996**, *1283*, 21.
(23) Bhattacharya, S.; Haldar, S. *Biochim. Biophys. Acta, Biomembr.* **2000**, *1467*, 39.
(24) Bhattacharya, S.; Bajaj, A. *J. Phys. Chem. B* **2007**, *111*, 2463.
(25) Bhattacharya, S.; Bajaj, A. *Langmuir* **2007**, *23*, 8988.
(26) Bhattacharya, S.; Biswas, J. *Langmuir* **2010**, *26*, 4642.
(27) Gordon, S. P.; Berezhna, S.; Scherfeld, D.; Kahya, N.; Schwille, P. *Biophys. J.* **2005**, *88*, 305.
(28) Ghosh, Y. K.; Visweswariah, S. S.; Bhattacharya, S. *Bioconjugate Chem.* **2002**, *13*, 378.
(29) Ghosh, Y. K.; Visweswariah, S. S.; Bhattacharya, S. *FEBS Lett.* **2000**, *473*, 341.
(30) Felgner, J. H.; Raj, K.; Sridhar, C. N.; Wheeler, C. J.; Tsai, Y. J.; Border, R.; Ramsey, P.; Martin, M.; Felgner, P. L. *J. Biol. Chem.* **1994**, *269*, 2550.
(31) Vist, M. R.; Davis, J. H. *Biochemistry* **1990**, *29*, 451.
(32) Ipsen, J. H.; Karlstrom, G.; Mouritsen, O. G.; Wennerstrom, H.; Zuckermann, M. G. *Biochim. Biophys. Acta* **1987**, *905*, 162.
(33) Presti, F. T.; Chan, S. I. *Biochemistry* **1982**, *21*, 321.
(34) Dufourc, E. J.; Parish, E. J.; Chitrakorn, S.; Smith, I. C. P. *Biochemistry* **1984**, *23*, 6062.
(35) Recktenwald, D. J.; McConnell, H. M. *Biochemistry* **1981**, *20*, 4505.
(36) Alecio, M. R.; Golan, D. E.; Veatch, W. R.; Rando, R. R. *Proc. Natl. Acad. Sci. U.S.A* **1982**, *79*, 5171.
(37) Smutzer, G.; Yeagle, P. *Biochim. Biophys. Acta* **1985**, *814*, 274.
(38) Van Ginkel, G.; Korstanje, L. J.; Van Langen, H.; Levine, Y. K. *Faraday Discuss. Chem. Soc.* **1986**, *81*, 49.
(39) Labrooke, B. D.; Williams, R. M.; Chapman, D. *Biochim. Biophys. Acta* **1968**, *150*, 333.
(40) Mabrey, S.; Mateo, P. L.; Sturtevant, J. L. *Biochemistry* **1978**, *17*, 2464.
(41) Sankaram, M. B.; Thompson, T. E. *Biochemistry* **1990**, *29*, 10676.
(42) Sankaram, M. B.; Thompson, T. E. *Proc. Natl. Acad. Sci. U.S.A.* **1991**, *88*, 8686.
(43) Bajaj, A.; Mishra, S. K.; Kondaiah, P.; Bhattacharya, S. *Biochim. Biophys. Acta* **2008**, *1778*, 1222.
(44) Hunter, R. J. *Zeta Potential Colloid Science*; Academic Press: New York, 1981.
(45) Bhattacharya, S.; Dileep, P. V. *J. Phys. Chem. B* **2003**, *107*, 3719.
(46) Bhattacharya, S.; Bajaj, A. *J. Phys. Chem. B* **2007**, *111*, 13511.
(47) Sturtevant, J. M. *Proc. Natl. Acad. Sci. U.S.A* **1982**, *79*, 3963.
(48) Hinz, H.-J.; Sturtevant, J. M. *J. Biol. Chem.* **1972**, *247*, 6071.
(49) Bhattacharya, S.; De, S. *Chem.—Eur. J.* **1999**, *5*, 2335.
(50) Bhattacharya, S.; De, S.; George, S. K. *Chem. Commun.* **1997**, 2287.
(51) Bhattacharya, S.; Ghosh, Y. K. *Langmuir* **2001**, *17*, 2067.
(52) Ghosh, Y. K.; Indi, S. S.; Bhattacharya, S. *J. Phys. Chem. B* **2001**, *105*, 10257.
(53) Bhattacharya, S.; Mandal, S. S. *Biochemistry* **1998**, *37*, 7764.

JP108372Z